Available online at www.sciencedirect.com
ScienceDirect
Journal of the European Ceramic Society 27 (2007) 585–592
www.elsevier.com/locate/jeurceramsoc

Nano-explosion synthesis of multi-component ceramic nano-composites

Oleg Vasylkiv [a,b,*], Yoshio Sakka [a], Valeriy V. Skorokhod [b]

[a] *National Institute for Materials Science, 1-2-1, Sengen, Tsukuba, Ibaraki, 305-0047, Japan*
[b] *Institute for Materials Science, NASU, 3, Krzhizhanivs'kogo Str., Kiev, 03680, Ukraine*

Available online 6 June 2006

Abstract

Here we demonstrate a unique processing technique which is based on engineering multi-component ceramic nanopowders and composites with precise morphology by nano-explosive deagglomeration/calcination. Multiple nano-explosions of impregnated cyclotrimethylene trinitramine deagglomerate the nanopowder due to the highly energetic impacts of the blast waves, while the solid-solubility of one component into the other is enhanced by the extremely high local temperature generated during the nano-explosions. We applied this technique to produce nanosize agglomerate-free ceria–gadolinia solid solution powder with uniform morphology and an average aggregate size of 32 nm, and 8 mol% yttria-doped zirconia aggregates with an average size of 53 nm impregnated with platinum (2–14 nm).

Keywords: Powders-chemical preparation; Calcination; Nanocomposites; CeO_2; ZrO_2

1. Introduction

Multi-component ceramic and metal–ceramic composite nanosize powders enable quality improvement and differentiation of product characteristics at scales currently unachievable by commercially available micron-, and submicron-size powders. Fabrication of nanopowders with uniform morphology and precise stoichiometry is a key to realizing high-performance devices based on nanostructured metal oxide ceramics for a wide range of applications.[1–3]

Nanopowders have previously been synthesized by so-called "wet chemical" methods from aqueous or non-aqueous solutions. A typical prior art synthesis procedure involves several sequential steps: (A) preparation of single- or multi-component starting solutions of metal salts (usually aqueous solutions); (B) preparation of aqueous solutions of different precipitants (reductants); (C) reductive decomposition of the starting single- or multi-component solution to obtain the precipitant, colloidal suspension or gel of the desired end-product phase or intermediate multi-component product; (D) separation of the end- (intermediate-) product; (E) deagglomeration of the synthesized (precipitated) powder prior to calcination; and (F) synthesis of the end-product powder via calcinations, i.e., thermal decomposition of the intermediate products.[1–19]

Due to the high surface energy and chemical activity of nanoparticles, aggregation and subsequent or simultaneous hard agglomeration are the main problems encountered in the preparation of such powders.[1–26] Despite these difficulties, several aqueous solution-based precipitation techniques have been employed to synthesize nanosize ceramic powders. These include the use of ammonia, oxalic acid, urea, ammonium carbonate and hexamethylenetetramine precipitants.[5–19] Preparation techniques have included approaches based on sol–gel processing,[5–26] reverse-micellar nanoreactor,[3,4] hydrothermal synthesis,[13–15] sonochemically and/or microwave-assisted decomposition of various aqueous (or non-aqueous) precursor solutions,[15] salt-assisted aerosol decomposition and combustion synthesis.[19–26]

However, processing multi-component fine powders has proven to be extremely challenging and usually results in a non-homogeneous multiphase compound with poor morphology.[2–16,19–23] Typically, nucleation, growth, aggregation and subsequent hard agglomeration of the first component occur within seconds under very mild conditions. The nucleation of the second component often starts at a higher temperature and requires more time and (very often) different pH. The final product of such "co-precipitation" is a non-homogeneous com-

* Corresponding author. Tel.: +81 29 851 3354x8820; fax: +81 29 860 4706.
E-mail address: oleg.vasylkiv@nims.go.jp (O. Vasylkiv).

0955-2219/$ – see front matter © 2006 Elsevier Ltd. All rights reserved.
doi:10.1016/j.jeurceramsoc.2006.04.157

posite powder, nanocrystalline in nature, but usually consisting of micrometer-size hard agglomerates with very poor morphology and composition homogeneity.[13] To achieve the desired solid solution, such a bi- or multi-component composite powder would require an excessive calcination temperature and unwarrantably prolonged holds.[6–15] Hence, it is not surprising that these powders also require high temperature and long soaking for densification, with no realistic prospect of achieving a fine-grained structure.[7–12]

The present study was aimed at establishing a non-traditional synthetic method of preparing nanosize, agglomerate-free, cerium–gadolinium oxide (CGO) ceramic powders with precise morphology and chemical composition. During the past decade, CeO_2-based materials have been intensively investigated as catalysts, structural and electronic promoters of heterogeneous catalytic reactions and oxide-ion conducting solid electrolytes in electrochemical cells.[10–12]

In addition, the possibility of engineering of 8Y-ZP/Pt composite nano-aggregates was also studied in this investigation. The addition of a metal to the ceramic matrix often produces a composite with more desirable properties than the individual components.[1,2,14–18] Nanometer-scaled clusters are very interesting in that their properties are between those of the condensed matter and atoms.[1–5] These clusters also provide excellent models for the study and understanding of surfaces and catalysis. We reported here, that Pt(II) ions were reduced from aqueous solutions of its salt onto the surface of the aggregated zirconia crystallites to form platinum nanoparticles impregnated into the zirconia (8Y-ZP) nano-aggregates.

In general, any explosive material is chemically or otherwise energetically unstable. Usually explosions involve a rapid and violent oxidation reaction with a sudden release of mechanical, chemical energy in a violent manner, accompanied with generation of high temperature and the release of extremely hot gases. It causes pressure waves in the local medium in which it occurs[25–27] Cyclotrimethylene trinitramine (RDX) – an explosive material in its pure synthesized state, it is a colorless crystalline solid with a density of 1.8 g/cm^3. It is a heterocycle and is thus ring-shaped with structural formula: hexahydro-1,3,5-trinitro-1,3,5-triazine or $(CH_2–N–NO_2)_3$.[20–27] At room temperature, it is extremely stable. Decomposition of RDX starts at about 170 °C, melting at 204 °C, and explosion at 233 °C (Table 1).

The method we describe here has no analogs and promises to become a principal player in advanced nano-technologies. It overcomes the main drawbacks, that is, agglomeration and compositional inhomogeneity,[1–3] of the numerous chemical methods of producing multi-component nanopowders – even those of combustion synthesis,[19–24] the method most closely related to ours.

Table 1
Characteristics of cyclotrimethylene trinitramine ($C_3H_6N_6O_6$)

Density	1.8 g/cm^3
Detonation rate	8350 m/s
Pressure at front of blast wave	33.8 GPa
Generated heat	
Burned	2.307 kcal/g
Exploded	1.3 kcal/g
Gas product volume	0.9 liter/g
Molecule size	0.48 nm

2. Experimental procedure

For the example (A) of our multiple nano-explosive synthesis method, $Ce(NO_3)_3{\cdot}6H_2O$, and $Gd(NO_3)_3{\cdot}6H_2O$ (both are 99.9% pure and produced by Wako Pure Chemicals Co., Osaka, Japan) were weighted and dissolved in demineralized water at a total concentration of 0.1 M (mol/L). The starting materials were used as received without further purification. The initial amount of cerium and gadolinium compounds varied according to the concentrations of both ceramics in the resulting composites.

To produce complex three-component intermediate agglomerates hexamethylenetetramine ($C_6H_{12}N_4$) (Wako Pure Chemicals Co., Osaka, Japan) was used as a precipitation agent and a source for cyclotrimethylene trinitramine (RDX) synthesis. Hexamethylenetetramine was dissolved in demineralized water at the concentration of 2.5 M/1 − x M of $Ce(NO_3)_3{\cdot}6H_2O$ and xM $GdCl_3{\cdot}6H_2O$. The total volume of the $C_6H_{12}N_4$ aqueous solution was 150 ml.

The complex three-component intermediate agglomerates were synthesized as-follows (five major steps):

(A1) Initial nucleation of gadolinium complex in the aqueous solution by spraying hexamethylenetetramine into gadolinium nitrate solution under the stirring conditions (1000–1600 rpm).

(A2) Suspension of gadolinium nitrate decomposition intermediate product was filled in a Teflon vessel and hydrothermaly treated at 110 °C for 7 h. The obtained homogeneous precipitate was hydrous gadolinia powder, which crystallized under hydrothermal conditions.

(A3) Washing with water, and subsequent redispersion of the gadolinia nanosized crystallites in distilled de-ionized water using an ultrasonic horn (Model USP-600, Shimadzu, Kyoto, Japan). The features of the ultrasonic re-dispersion have been well-described earlier for de-agglomeration of hydrothermally prepared yttria-stabilized zirconia nanosized powders.[14] Low-temperature (2 °C) mixing of the aqueous suspension of gadolinia with aqueous solution of cerium nitrate hexahydrate under the stirring conditions of 1000–1600 rpm. To maintain the constant temperature of 2 °C, the mixing was carried out in a temperature controlled water bath.

(A4) The stock suspension was mixed (1000–1600 rpm) using a magnetic stirrer at 90 °C for a prescribed time. Subsequently, the composite powder (i.e., three component intermediate agglomerates) was separated from the supernatant by centrifuging (10 000 rpm for 15–20 min). The composite powders were then washed several times with distilled and de-ionized water to remove the residual reaction products. Washing with water was followed by ethanol (C_2H_5OH, 99.5% reagent grade, Kanto Chemicals, Japan) washing with subsequent centrifuging, re-dispersing in fresh ethanol and then a final slow evaporation of the ethanol (T = 70 °C) using a drying oven.

Mixing hexamethylenetetramine with nitric acid directly or after decomposition of its salts into the aqueous stock solutions of nitrates causes the formation and precipitation of cyclotrimethylene trinitramine ($C_3H_6N_6O_6$) with simultaneous saturation (nano-level impregnation) into the matrix of the bi-component precursor agglomerates (matrix cerium–gadolinium composite agglomerates).

(A5) Multiple nano-explosive calcination/deagglomeration of ceria–gadolinia solid solution.

For the example (B), $ZrO(NO_3)_2{\cdot}nH_2O$ (99.9% pure and produced by Wako Pure Chemicals Co., Japan), and YCl_3 produced as described elsewhere[14] were weighted and dissolved in water at a total concentration of 0.1 M. The initial amount of zirconium and yttrium compounds varied according to the concentrations of both compounds in the resulting composites. The preparation conditions of the 8Y-ZP nanopowder were well described in earlier paper.[14] However, hexamethylenetetramine was used instead of urea as a precipitation agent in present study. Reagent-grade potassium tetrachloroplatinate (K_2PtCl_4) (produced by Wako Pure Chemicals Co., Osaka, Japan) was used as a platinum source. K_2PtCl_4 stock aqueous solutions was initially prepared and aged for 12 h at 20 °C. The initial amount of Pt compound varied according to the final concentration of metal in the metal–ceramic composites between 5 and 10 wt.%.

Similar to the example (A) after hydrothermal treatment and washing the homogeneously precipitated hydrous 8Y-ZP powder was redispersed in water and subsequently mixed with potassium tetrachloroplatinate aqueous solution. The suspension was mixed using a magnetic stirrer with heating (150 °C) for a prescribed time. Subsequently, the three-component powder agglomerates (hydrous 8Y-ZP, Pt clusters and RDX) were separated from the supernatant by centrifuging (10 000 rpm for 15–20 min) as described in previous paper.[15]

RDX (synthesized separately), complex precursor powder of cerium and gadolinium compound and hydrous zirconia were tested for decomposition using thermogravimetric and differential thermal analysis (TG-DTA) (Thermo Plus 2 Rigaku, TG8120, Japan). The reference used for the DTA was an Al_2O_3 sample, the sample containers in the equipment were alumina, and an atmosphere O_2/N_2 was used. Heating rates of 5–30 °C/min, were used. Isothermal holdings and changes of the reaction atmosphere were not applied in this study. The TG-DTA experiments were used to determine the calcination conditions versus heating rate dependence.

The particle-size distribution was analyzed by dynamic light scattering method (DLS) using a laser particle-size analyzer (Model LSPZ-100, Otsuka Electronics, Osaka, Japan). A very small amount of each powder (≤5 mg) was dispersed in the distilled water for the analysis. Observation via TEM (Model JEM-2100-F, JEOL, Tokyo, Japan) operated at 200 kV was used to determine the powder morphology. Phase identification of the powders and distribution of the components into each aggregate were determined by nano-area energy dispersion X-ray spectroscopy analyzer (TEM-EDX), and from X-ray diffractometry data (XRD) (Model RINT 2000, Rigaku, Tokyo, Japan). The XRD profiles were recorded using Cu$K\alpha$ radiation under 40 kV and 300 mA at room temperature.

Table 2
The particle size (aggregates and agglomerates size) distribution for gadolinia, as synthesized, and subsequently hydrothermaly treated at 110 °C

Time of hydrothermal treatment, hours	Particles size distribution, nm	Particles size distribution after ultrasonic deaglomeration during 100 s, nm
No treatment	4–340	4–310
7	3–218	3–21

3. Results and discussion

3.1. Nano-explosive calcination/deagglomeration of ceria–gadolinia powder

Synthesis of the gadolinium oxide in the aqueous solution by spraying hexamethylenetetramine into the gadolinium chloride solution with subsequent hydrothermal treatment at 110 °C was performed prior to the ceria synthesis. The particle size distribution (both aggregate and agglomerate) of gadolinia powders, as synthesized, and subsequently hydrothermaly treated at 110 °C are shown in Table 2. As-synthesized gadolinia powder consists of agglomerated primary particles (3–4 nm) with agglomerate size distribution of 4–310 nm. No significant influence of ultrasonic treatment on powder agglomerates was detected. The optimum conditions of hydrothermal treatment of 7 h at 110 °C have produced the hydrous gadolinia powder with the aggregate/agglomerate size distribution of 3–218 nm. However, the short-term ultrasonic treatment leads to the significant de-agglomeration of the hydrolyzed powder. Gadolinia hydrous powder with aggregate size distribution of 3–21 nm (after ultrasonic de-agglomeration during 100 s) was produced (Table 2).

The stock suspension of gadolinia hydrous particles in the cerium nitrate aqueous solution and hehamethylenetetramine was heated at 90 °C for required time. The primary particles of gadolinia assembled into agglomerates covered with as-synthesized ceria. Table 3 shows the size distribution of the engineered complex precursor agglomerates (gadolinia-doped ceria particles with RDX) as analyzed by dynamic light scattering (DLS). The composite powder agglomerates ranged in size from 27–239 nm.

A diagram of the processing pathway is shown in Fig. 1. Well-dried powder composed of the complex precursor agglomerates was briquetted by uniaxial pressing and filled into an alumina container for further thermal treatment. A governing factor behind our methodology is to prevent the undesirable igni-

Table 3
Powders aggregate/agglomerate size distribution for complex precursor agglomerates of gadolinia-doped ceria with RDX (A), and 8Y-ZP/Pt (B), as synthesized, after multiple nano-explosion calcinations/deagglomeration; and, finally, after subsequent non-isothermal calcination up to 450 °C

Composition	As-synthesized complex precursor agglomerates (nm)	After multiple explosive treatment (nm)	After calcination up to 450 °C (nm)
CGO (A)	27–239	15–47	15–52
8Y-ZP/Pt (B)	9–347	17–79	24–83

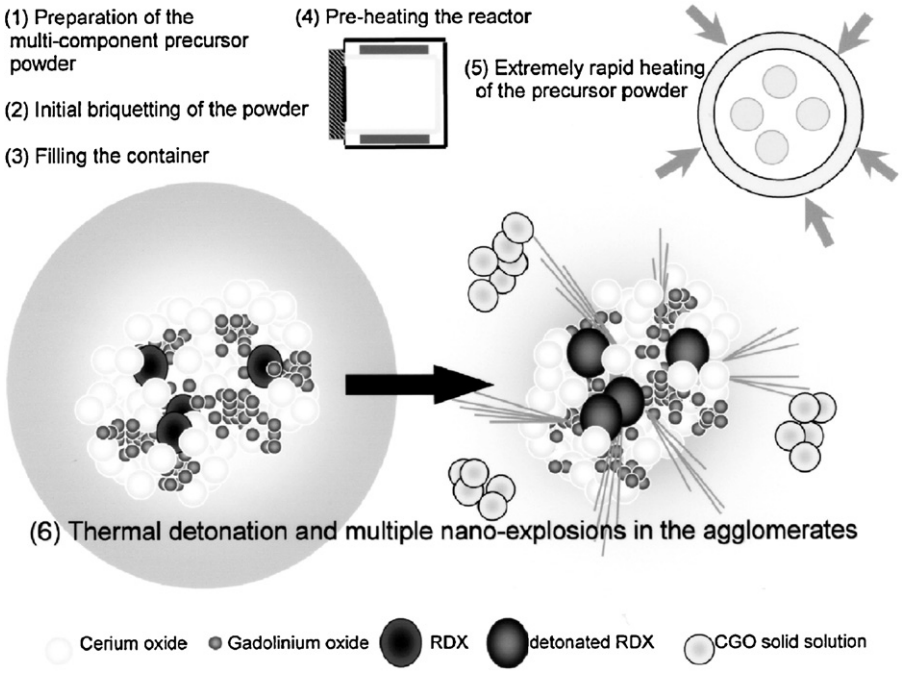

Fig. 1. Diagram of the processing pathway.

tion of the RDX by ultra-rapid heating of the multi-component complex agglomerate through thermal detonation temperature (~230 °C for RDX). This thermal detonation temperature, i.e., the temperature at which spontaneous multiple ruptures of the N–NO_2 bonds occur, strongly depends on the heating rate and may vary from 220 to 360 °C. As with other explosives, the explosive initiation of RDX begins in nanosize regions – so-called "hot spots" – which are capable of accumulating the mechanical energy of an impact/shock wave and transferring it into chemical energy, thus starting the blast reaction. Cleavage of the N–NO_2 chemical bonds requires less energy for isolated molecules (or clusters) than for molecules located in the bulk of the solid. Extremely rapid detonation (10^{-8} s/gram) forms gaseous products with a temperature of 2000–5000 °C compressed into a volume equaling the initial volume of each explosive RDX particle. Multiple nano-explosions occur within the volume of the multi-component precursor agglomerates. The instantaneous power of each explosion (i.e., the expansion of compressed gases) is 500 MW/gram.[25–27] The impacts of the blast waves lead to the crushing, defragmentation and plastic deformation of the surrounding matter. The rapid evolution of a large volume of gaseous products during combustion dissipates the heat of the process and limits temperature increase, thus reducing the possibility of premature local partial sintering among the primary particles. This gas evolution also helps by somewhat limiting inter-particle contact resulting in a less-agglomerated product. Multi-explosive deagglomeration of the nanopowder occurred due to the highly energetic impact of the blast waves, while the short-term high temperature generated during the explosions enhanced the solid-solubility of one component into the other. Nanosize bi-metal (cerium and gadolinium) oxide composite and, very soon afterwards, a solid solution of the dopant oxide (gadolinia) into the matrix oxide (ceria) were synthesized. Utilizing the methodology described here, we produced cerium–gadolinium oxide (CGO) powder with an average primary crystallite size of 9 nm, an aggregate size distribution of 15–52 nm (see Table 3), uniform morphology and precise stoichiometry.

We analyzed the thermal decomposition of both RDX itself (Fig. 2) and of RDX distributed within the complex precursor agglomerates of cerium–gadolinium compounds produced under both rapid (Fig. 3) and slow (Fig. 4) heating conditions. This enabled us to identify the explosive decomposition conditions of the RDX synthesized together with the cerium and gadolinium and simultaneously impregnated onto intermediate precursor agglomerates, and confirm them by comparison with the explosive decomposition conditions of RDX itself. Results for thermogravimetric (TG) and differential thermal analysis (DTA) of the thermal explosion of RDX itself under super-critical conditions (heating rate = 10 °C/min or higher) are

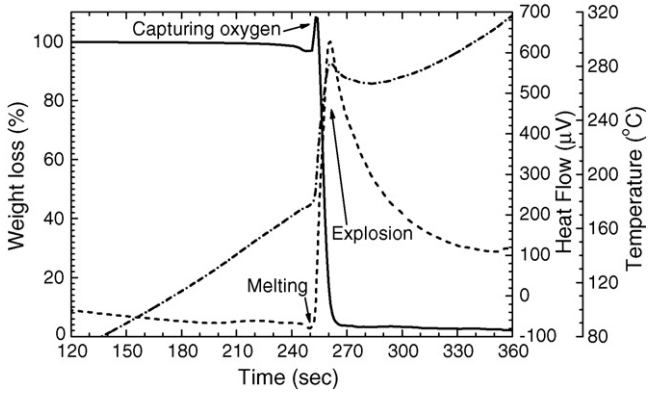

Fig. 2. TG/DTA analysis of the thermal explosion of RDX (heating rate = 20 °C/min, solid line: TG, dash line: DTA, and dash dot line: temperature).

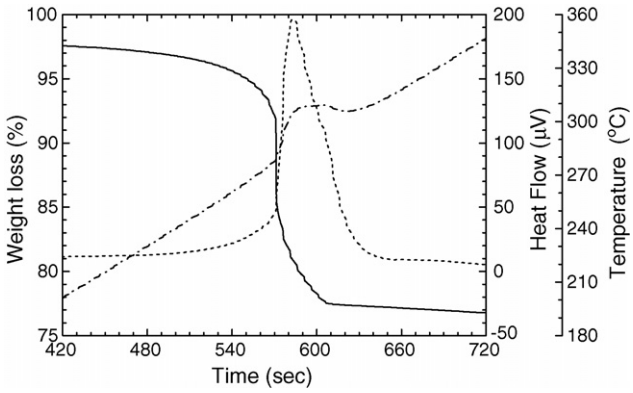

Fig. 3. TG/DTA analysis of the thermal explosion of RDX during the multi-explosive synthesis of ceria–gadolinia solid solution (heating rate = 20 °C/min, solid line: TG, dash line: DTA, and dash dot line: temperature).

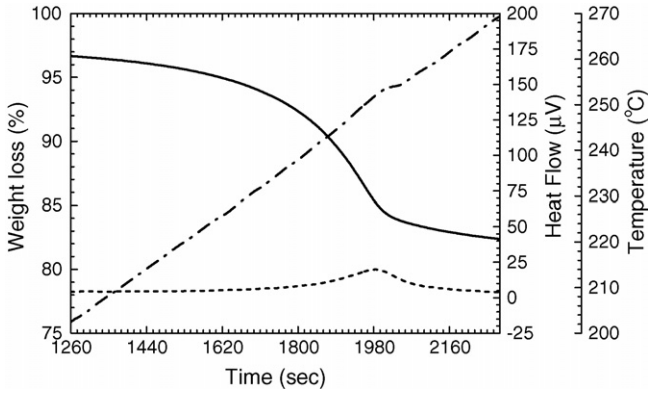

Fig. 4. TG/DTA analysis of the thermal decomposition of the multi-component precursor complex under sub-critical conditions (heating rate = 5 °C/min, solid line: TG, dash line: DTA, and dash dot line: temperature).

shown in Fig. 2. Three stages can be identified in the thermal decomposition. At the heating rate of 20 °C/min, the ignition of the RDX started at around 180 °C. The ignition temperature depended directly on the heating rate: the higher the heating rate used, the smaller was the gap between the theoretical (∼180 °C) and the experimentally measured ignition temperature. 202–205 °C is the melting point of RDX. A slight endothermic peak can be detected irrespective of the extremely short melting time (2 s for the RDX particles filled into the container with no preliminary densification) prior to the explosion. The thermal explosion of the RDX occurred at ∼230 °C. Just at the beginning of the ignition reaction, the TG analysis detected a significant increase in the mass of the sample (approximately 10.8 wt.% at the heating rate of exactly 20 °C/min.). This phenomenon is explained by the capturing of external oxygen from neighboring space by the reacting species. The ignition instantly (within nanoseconds) transformed into thermal detonation, i.e., the RDX exploded. Even the temperature as detected by the thermocouple of the TG/DTA system momentarily increased by about 100 °C.

Fig. 3 shows TG-DTA analysis results for the thermal explosion of RDX during the thermal decomposition of multi-component precursor complex agglomerates under super-critical conditions with a heating rate of 20 °C/min. The reaction results observed here are not, however, limited to this particular rate. The strong exothermal peak detected by differential thermal analysis at similar temperature and time as for RDX itself (seen in Fig. 2) confirms the occurrence of multiple nano-explosions of RDX uniformly distributed into the volume of the multi-component precursor agglomerates.

TG-DTA analysis results for the thermal decomposition of the multi-component precursor complex under sub-critical conditions with a heating rate of 5 °C/min are shown in Fig. 4.

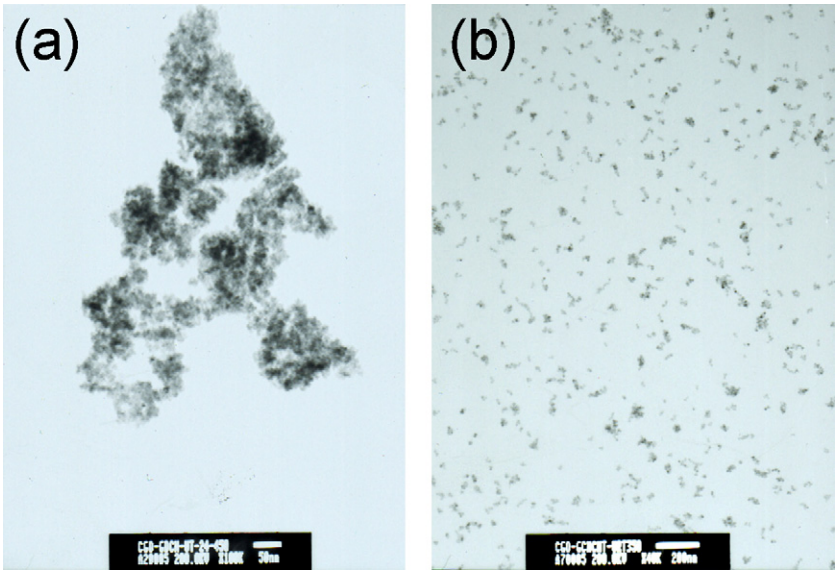

Fig. 5. TEM micrograph of ceria–gadolinia composite agglomerates (a) produced under sub-critical conditions (i.e., at a sub-critical rate with calcination to 450 °C), and (b) micrograph of cerium–gadolinium oxide (CGO) nano-aggregates produced with applying the nano-explosive synthesis method.

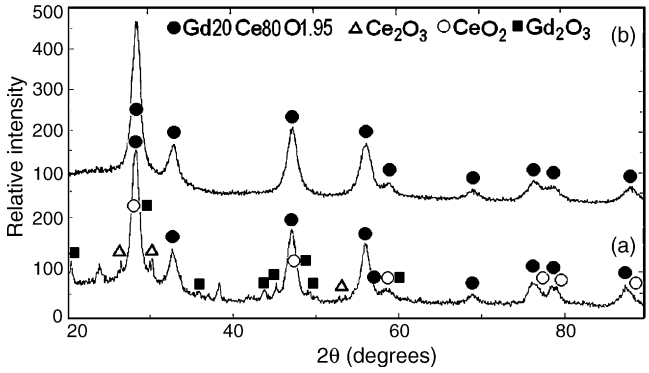

Fig. 6. XRD patterns of (a) a ceria–gadolinia composite nanopowder produced under sub-critical conditions (seen in Fig. 5), and (b) a ceria–gadolinia solid solution synthesized by the multiple nano-explosion method.

There is no significant exothermal peak in the DTA curve. We can assume that the sub-critical temperature/time conditions prevented multiple thermal detonations in the hot spots, and, consequently, only slow burning of the RDX occurred. Under such sub-critical conditions, this method may be considered as a combustion route. Fig. 5a shows a transmission electron microscope micrograph of the ceria–gadolinia composite agglomerates produced without applying nano-explosive synthesis method (i.e., under sub-critical temperature/time conditions with following calcination to 450 °C). Agglomerates of very fine primary crystallites of gadolinia appear in the TEM image as large, black, non-uniform particles. Nano-area TEM-energy dispersive X-ray (EDX) spectra of these composite nano-aggregates synthesized by the combustion route under sub-critical conditions show the existence of both cerium and gadolinium inside the aggregates (not shown here, because the lack of space). Nano-aggregates of a ceria–gadolinia solid solution synthesized by the multiple nano-explosive method are shown in the TEM micrograph in Fig. 5b. Fig. 6 shows XRD patterns of (a) the ceria–gadolinia composite nanopowder produced by the combustion route under sub-critical conditions, and (b) the ceria–gadolinia solid solution produced by multiple nano-explosive synthesis. In (b), the weak reflections associated with Ce_2O_3 and Gd_2O_3 have disappeared. Moreover, the XRD peaks attributed to the Gd20Ce80O1.95

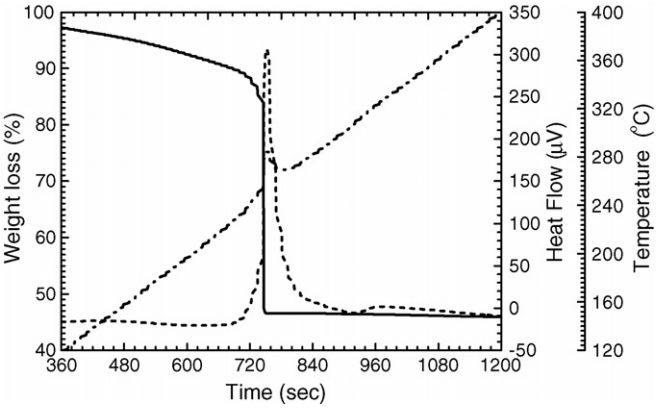

Fig. 7. TG/DTA analysis of the thermal explosion of RDX during the multi-explosive calcination of 8Y-ZP/Pt powder (heating rate = 20 °C/min, solid line: TG, dash line: DTA, and dash dot line: temperature).

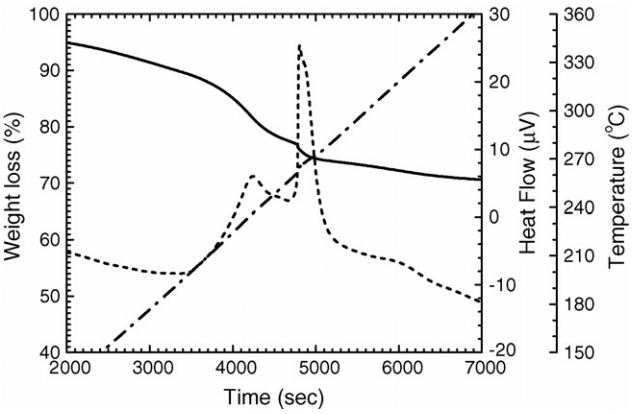

Fig. 8. TG/DTA analysis of 8Y-ZP/Pt powder calcination under sub-critical conditions (heating rate = 5 °C/min, solid line: TG, dash line: DTA, and dash dot line: temperature).

composite are relatively broad indicating that the powder is composed of very fine crystallites. Subsequent non-isothermal calcination up to 350–450 °C may lead to removal of the products of the explosive decomposition of RDX. Thus, such treatment acts to preserve both the powder's compositional homogeneity and morphology.

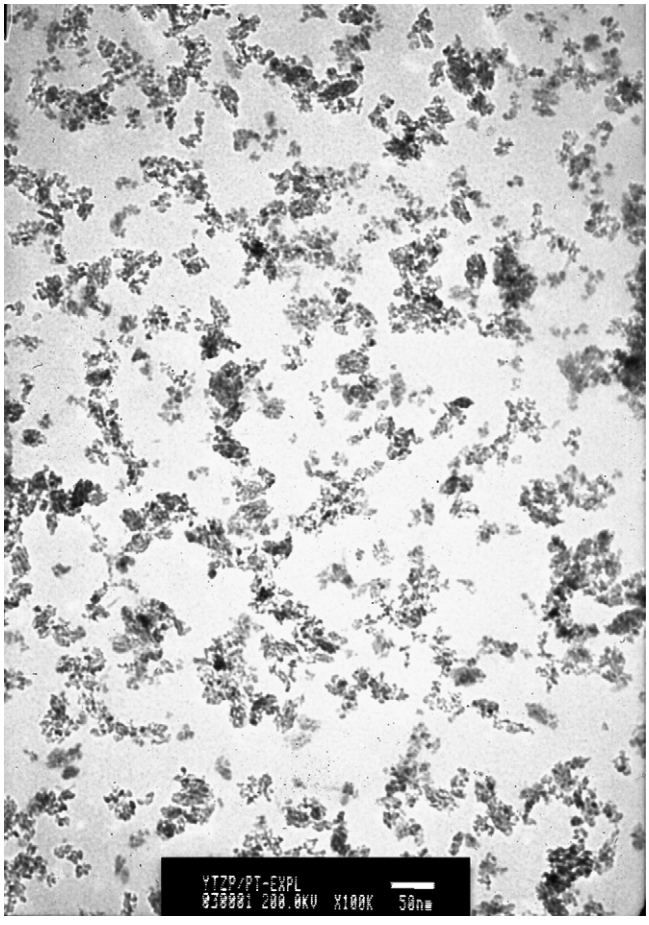

Fig. 9. TEM micrograph of 8Y-ZP/Pt composite nano-aggregates produced with applying the nano-explosive synthesis method.

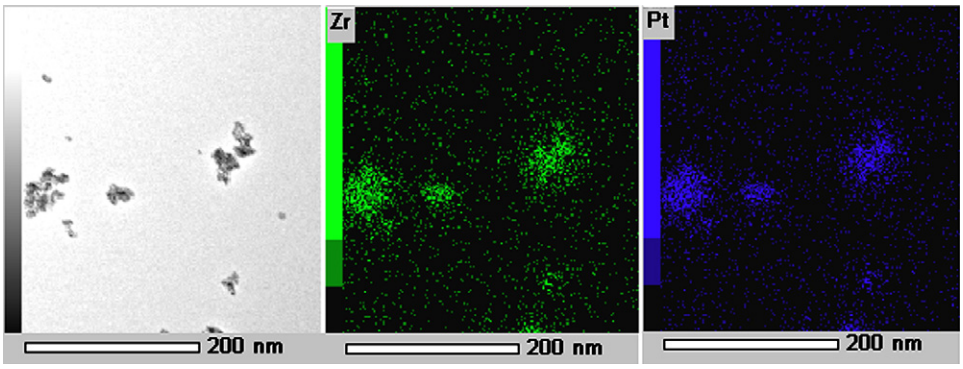

Fig. 10. The TEM-EDX mapping of 8Y-ZP/Pt aggregates.

3.2. Nano-explosive calcination of 8Y-ZP/Pt composite

The aqueous suspension of hydrothermaly treated 8Y-ZP powder agglomerates (9–347 nm) embedded with RDX was mixed with K_2PtCl_4 aqueous solution. Subsequent thermal reduction of the platinum compounds was applied. The beaker with the suspension was heated using the temperature-controlled heater of a magnet stirrer. During 5 h, the color of the mixed suspensions of the hydrothermaly treated 8Y-ZP nanopowder disperced within an aqueous solution of K_2PtCl_4 changed from yellow to white through light gray to dark-gray. The fine (2–7 nm) platinum particles were reduced on the surface of the 8Y-ZP nano-aggregates.

We analyzed the thermal decomposition of complex precursor agglomerates of hydrous 8Y-ZP with platinum clasters and impregnated with RDX under both rapid (Fig. 7) and slow (Fig. 8) heating conditions. Fig. 7 shows TG-DTA analysis results for the thermal explosion of RDX during the calcination of 8Y-ZP/Pt composite powder under super-critical conditions with a heating rate of 20 °C/min. The reaction results observed here are also not limited to this particular rate. The strong exothermal peak detected by differential thermal analysis at similar temperature and time as for RDX itself (seen in Fig. 2) and cerium–gadolinium compound with RDX (Fig. 3) confirms the occurrence of multiple nano-explosions of RDX distributed within 8Y-ZP/Pt composite agglomerates.

TG-DTA analysis results for the calcination of 8Y-ZP/Pt composite powder under sub-critical conditions with a heating rate of 5 °C/min are shown in Fig. 8. There are two weak exothermal peaks in the DTA curve. The first one was attributed to the ignition of RDX particles and the second one confirms that some amount of RDX was able to explode even the most of it already burned at lower temperature. However, we can assume that under the sub-critical temperature/time conditions mostly ignition and subsequent combustion of the RDX occurred.

A TEM micrograph of the 8 mol% yttria-stabilized zirconia (8Y-ZP) nano-powder is shown in Fig. 9. The primary crystallites with an average size of ~8 nm are aggregated into secondary nano-aggregates with a mean aggregate size of 24–83 nm. The TEM-EDX mapping image of 8Y-ZP/Pt aggregates (Fig. 10) shows the uniform distribution of platinum particles within the zirconia aggregates.

4. Conclusion

The fabrication of nanopowders with uniform morphology and precise stoichiometry is key to realizing high-performance devices based on nanostructured metal oxide ceramics and metal-ceramic composites for a wide range of applications. Here we demonstrate a unique processing technique which is based on engineering multi-component ceramic nanopowder with precise morphology by multiple nano-blast deagglomeration/calcination. Multiple nano-explosions of impregnated RDX deagglomerate the nanopowder due to the highly energetic impacts of the blast waves. Solid-solubility of one component into the other is enhanced by the extremely high local temperature generated during the nano-explosions. We produced nanosize agglomerate-free ceria-gadolinia powder with excellent morphology and an average aggregate size of 32 nm. In addition, Pt nano-particles (2–14 nm) were impregnated into zirconia (8Y-ZP) nano-aggregates (24–83 nm) and powder was calcined/deagglomerated by this technique. The described method opens the door to the synthesis of a wide range of multi-metal oxide ceramics and metal–ceramic composite nanopowders with uniform morphology and precise stoichiometry.

Acknowledgements

This study was performed through Special Coordination Funds for Promoting Science and Technology from the Ministry of Education, Culture, Sports, Science and Technology of the Japanese Government.

References

1. Gleiter, H., Nanocrystalline materials: basic concept and microstructure. *Acta Mater.*, 2000, **48**, 1–29.
2. Tjong, S. and Chen, H., Nanocrystalline materials and coatings. *Mater. Sci. Eng. R.*, 2004, **45**, 1–88.
3. Johnston, K. and Shah, P., Making nanoscale materials with supercritical fluids. *Science*, 2004, **303**, 482–483.
4. Pileni, M.-P., The role of soft colloidal templates in controlling the size and shape of inorganic nanocrystals. *Nat. Mater.*, 2003, **2**, 145–150.
5. Millman, J., Bhatt, K., Prevo, B. and Velev, O., Anisotropic particle synthesis in dielectrophoretically controlled microdroplet reactors. *Nat. Mater.*, 2005, **4**, 98–102.

6. Lee, J.-S. and Choi, S.-C., Crystallization behavior of nano-ceria powders by hydrothermal synthesis using a mixture of H_2O_2 and NH_4OH. *Mater. Lett.*, 2004, **58**, 390–393.
7. Vasylkiv, O. and Sakka, Y., Synthesis and sintering of zirconia nanopowder by non-isothermal decomposition from hydroxide. *J. Ceram. Soc. Japan*, 2001, **109**, 500–505.
8. Vasylkiv, O. and Sakka, Y., Non-isothermal synthesis of yttria-stabilized zirconia nanopowder through oxalate processing: I. Characteristics of (Y-Zr) oxalate synthesis and its decomposition. *J. Am. Ceram. Soc.*, 2000, **83**, 2196–2202.
9. Vasylkiv, O., Sakka, Y. and Borodians'ka, H., Non-isothermal synthesis of yttria-stabilized zirconia nanopowder through oxalate processing: I. Morphology manipulation. *J. Am. Ceram. Soc.*, 2001, **84**, 2484–2488.
10. Tianshu, Z., Hing, P., Huang, H. and Kilner, J., Ionic conductivity in the CeO_2–Gd_2O_3 system ($0.05 \leq Gd/Ce \leq 0.4$) prepared by oxalate co-precipitation. *Solid State Ionics*, 2002, **148**, 567–573.
11. Li, J.-G., Ikegami, T., Wang, Y. and Mori, T., $Ce_{1-x}Y_xO_{2-x/2}$ ($0 \leq x \leq 0.35$) oxides via carbonate precipitation: synthesis and characterization. *Solid State Chem.*, 2002, **168**, 52–59.
12. Zhang, T., Ma, J., Kong, L., Hing, P. and Kilner, J., Preparation and mechanical properties of dense $Ce_{0.8}Gd_{0.2}O_{2-\delta}$ ceramics. *Solid State Ionics*, 2004, **167**, 191–196.
13. Vasylkiv, O., Kolodiazhni, T., Sakka, Y. and Skorokhod, V., Synthesis and characterization of nanosize ceria–gadolinia powders. *J. Ceram. Soc. Japan*, 2005, **113**, 101–106.
14. Vasylkiv, O. and Sakka, Y., Synthesis and colloidal processing of zirconia nanopowder. *J. Am. Ceram. Soc.*, 2001, **84**, 2489–2494.
15. Vasylkiv, O., Sakka, Y., Maeda, Y. and Skorokhod, V., Nano-engineering of zirconia-noble metals composites. *J. Eur. Ceram. Soc.*, 2004, **24**, 469–473.
16. Chen, Y.-Z., Liaw, B.-J., Kao, C.-F. and Kuo, J.-C., Yttraia-stabilized zirconia supported platinum catalysts (Pt/YSZs) for CH_4/CO_2 reforming. *Appl. Catal. A: Gen.*, 2001, **217**, 23–31.
17. Hendriks, M., Boukamp, B., Elshof, J., van Zyl, W. and Verweij, H., The electrical behaviour of platinum impregnated porous YSZ. *Solid State Ionics*, 2002, **146**, 123–132.
18. Hendriks, M., van Zyl, W., Elshof, J. and Verweij, H., Capacitance at ambient temperature and microstructure of platinum/yttria-stabilized zirconia composites. *Mater. Res. Bull.*, 2001, **36**, 2395–2406.
19. Wu, N.-L., Wang, S.-Y. and Rusakova, I. A., Ingibition of crystallite growth in the sol-gel synthesis of nanocrystalline metal oxides. *Science*, 1999, **285**, 1375–1377.
20. Ulrich, G., Flame synthesis of fine particles. *Chem. Eng. News*, 1998, **62**, 22–29.
21. Pratsinis, S., Flame aerosol synthesis of ceramic powders. *Prog. Energy Combust. Sci.*, 1998, **24**, 197–219.
22. Sorensen, C., Hageman, W., Rush, T., Huang, H. and Oh, C., Aerogelation in a flame soot aerosol. *Phys. Rev. Lett.*, 1998, **80**, 1782–1785.
23. Purohit, R., Sharma, B., Pillai, K. and Tyagi, A., Ultrafine ceria powders via glycine-nitrate combustion. *Mater. Res. Bull.*, 2001, **36**, 2711–2721.
24. Varma, A. and Lebrat, J.-P., Combustion synthesis of advanced materials. *Chem. Eng. Sci.*, 1992, **47**, 2179–2196.
25. Tillotson, T., Hrubesh, L., Simpson, R., Lee, R., Swansiger, R. and Simpson, L., Sol–gel processing of energetic materials. *J. Non-Cryst. Solids*, 1998, **225**, 358–363.
26. Tillotson, T., Gash, A., Simpson, R., Hrubesh, J., Satcher, L., Poco Jr. and Poco, J., Nanostructured energetic materials using sol–gel methodologies. *J. Non-Cryst. Solids*, 2001, **285**, 338–345.
27. Kuklja, M., Thermal decomposition of solid cyclotrimethylene trinitramine. *J. Phys. Chem. B*, 2001, **105**, 10159–10162.